

# HEAT-TRANSFER CHARACTERISTICS OF A NON-NEWTONIAN Au NANOFUID IN A CUBICAL ENCLOSURE WITH DIFFERENTIALLY HEATED SIDE WALLS

## ZNAČILNOSTI PRENOSA TOPLOTE NENEWTONSKE Au NANOTEKOČINE V KOCKASTEM OHIŠJU Z RAZLIČNO GRETIMA STRANSKIMA STENAMA

Primož Ternik<sup>1</sup>, Rebeka Rudolf<sup>2,3</sup>, Zoran Žunič<sup>4</sup>

<sup>1</sup>Private Researcher, Bresterniška ulica 163, 2354 Bresternica, Slovenia

<sup>2</sup>University of Maribor, Faculty of Mechanical Engineering, Smetanova 17, 2000 Maribor, Slovenia

<sup>3</sup>Zlatarna Celje, d. d., Keršnikova ul.19, 3000 Celje, Slovenia

<sup>4</sup>AVL-AST, Trg Leona Štuklja 5, 2000 Maribor, Slovenia  
pternik@pt-rtd.eu

*Prejem rokopisa – received: 2013-10-14; sprejem za objavo – accepted for publication: 2014-02-17*

The present work deals with the laminar natural convection in a cubical cavity filled with a homogenous aqueous solution of carboxymethyl cellulose (CMC) based gold (Au) nanofluid obeying the power-law rheological model. The cavity is heated on the vertical and cooled from the adjacent wall, while the other walls are adiabatic. The governing differential equations were solved with the standard finite-volume method and the hydrodynamic and thermal fields are coupled using the Boussinesq approximation.

The main objective of this study is to investigate the influence of the nanoparticle volume fraction on the heat-transfer characteristics of CMC-based Au nanofluid over a wide range of the base-fluid Rayleigh number.

Accurate numerical results are presented in the form of dimensionless temperature and velocity variations, the mean Nusselt number and the heat-transfer rate. It is shown that adding nanoparticles to the base fluid delays the onset of natural convection. In addition, numerical simulations showed that, just after the onset of natural convection, adding nanoparticles reduces the mean Nusselt number value for any given base-fluid Rayleigh number.

Keywords: natural convection, CMC-Au nanofluid, heat transfer, Nusselt number

Prispevek obravnava naravno konvekcijo v kockastem ohišju, napolnjenem s homogeno nanotekočino karboksimetil celuloza (CMC)-zlato (Au), z reološkim vedenjem, opisanim s potenčnim zakonom. Ohišje je greto na navpični in hlajeno na priležni steni, medtem ko so druge stene adiabatne. Vodilne diferencialne enačbe so bile rešene s standardno metodo končnih prostornin, pri čemer sta hidrodinamično in temperaturno polje sklopljena z Boussinesqovo aproksimacijo.

Glavni cilj prispevka je raziskati vpliv prostorninskega deleža nanodelcev na značilnosti prenosa toplote CMC-Au nanotekočine za široko območje vrednosti Rayleighjevega števila nosilne tekočine.

Natančni rezultati so predstavljeni v obliki spreminjanja brezdimenzijske temperature in hitrosti, srednje vrednosti Nusseltovega števila in hitrosti prenosa toplote. Pokazano je, da dodajanje nanodelcev v nosilno tekočino zakasni začetek naravne konvekcije. Poleg tega so numerične simulacije pokazale, da takoj za pojavom naravne konvekcije dodajanje nanodelcev zmanjšuje srednjo vrednost Nusseltovega števila za katero koli vrednost Rayleighjevega števila nosilne tekočine.

Gljučne besede: naravna konvekcija, nanotekočina CMC-Au, prenos toplote, Nusseltovo število

## 1 INTRODUCTION

In recent years, nanosized particles dispersed in a base fluid, known as nanofluid<sup>1</sup>, have been used and researched extensively to enhance the heat transfer in many engineering applications. While the presence of nanoparticles shows an unquestionable heat-transfer enhancement in forced-convection applications<sup>2</sup> there is still a dispute on the influence of nanoparticles on the heat-transfer enhancement of a buoyancy-driven flow.

Natural convection (i.e., a flow caused by temperature-induced density variations) is one of the most extensively analysed configurations because of its fundamental importance as the "benchmark" problem for studying convection effects (and comparing as well as validating numerical techniques). In addition to the obvious academic interest, a thermally driven flow is the strategy preferred by heat-transfer designers when a small power

consumption, a negligible operating noise and a high reliability of a system are the main concerns (e.g., a reduction of the cooling time, manufacturing cost and an improvement of the product quality in the injection-moulding industry<sup>3</sup>). Although various configurations of the enclosure problem are possible<sup>4-8</sup>, one of the most studied cases (involving nanofluids) is a two-dimensional square enclosure with differentially heated isothermal vertical walls and adiabatic horizontal walls<sup>9-11</sup>. Recent numerical studies<sup>12,13</sup> illustrated that the suspended nanoparticles substantially increase the heat-transfer rate for any given Rayleigh number. In addition, it is shown that the heat-transfer rate in water-based nanofluids increases with an increasing volume fraction of Al<sub>2</sub>O<sub>3</sub>, Cu, TiO<sub>2</sub> or Au nanoparticles. On the other hand, an apparently paradoxical behaviour of the heat-transfer deterioration was observed in many experimen-

tal studies: e.g., Putra et al.<sup>14</sup> reported that the presence of Al<sub>2</sub>O<sub>3</sub> nanoparticles in a base fluid reduces the natural-convective heat transfer. However, they did not clearly explain why the natural-convective heat transfer decreases with an increase in the volume fraction of nanoparticles. This was later explained by the work of Ternik and Rudolf<sup>4</sup>.

Regarding the natural convection in a 3D cubic cavity, most (if not all) of the work was done for the Newtonian fluid. For example, Tric et al.<sup>15</sup> studied the natural convection in a 3D cubic enclosure using a pseudo-spectra Chebyshev algorithm based on the projection-diffusion method with the spatial resolution supplied by polynomial expansions. Lo et al.<sup>16</sup> also studied the same problem under different inclination angles using the differential-quadrature method to solve the velocity-vorticity formulation of the Navier-Stokes equation employing higher-order polynomials to approximate differential operators.

The above review of the existing literature shows that the problem of natural convection in a cubical cavity filled with a nanofluid is an issue still far from being tackled and solved. Framed in this general background, the purpose of the present study is to examine the effect of adding Au nanoparticles to a non-Newtonian base fluid on the conduction and convection heat-transfer characteristics in a differentially heated cubical cavity heated over a wide range of the base-fluid Rayleigh number ( $10^1 \leq Ra_{bf} \leq 10^6$ ) and the volume fraction of nanoparticles ( $0 \% \leq \varphi \leq 10 \%$ ).

## 2 NUMERICAL MODELLING

The standard finite-volume method is used to solve the coupled conservation equations of mass, momentum and energy. In this framework, a second-order central differencing scheme is used for the diffusive terms and a second-order upwind scheme for the convective terms. The coupling of the pressure and velocity is achieved using the SIMPLE algorithm. The convergence criteria were set to  $10^{-8}$  for all the relative (scaled) residuals.

### 2.1 Governing equations

For the present study, a steady-state flow of an incompressible non-Newtonian CMC-Au nanofluid is considered. It is assumed that both the fluid phase and nanoparticles are in thermal and chemical equilibrium. Except for the density, the properties of the nanoparticles and the fluid (presented in **Table 1**) are taken to be constant. The Boussinesq approximation is invoked for the nanofluid properties to relate the density changes to the temperature changes, and to couple the temperature field with the velocity field.

The governing equations (mass, momentum and energy conservation) of such a flow are<sup>9</sup>:

$$\frac{\partial v_i}{\partial x_i} = 0 \tag{1}$$

$$\rho_{nf} v_j \frac{\partial v_i}{\partial x_j} - \frac{\partial}{\partial x_j} \left( \eta_{nf} (|\dot{\gamma}|) \frac{\partial v_i}{\partial x_j} \right) = -\frac{\partial p}{\partial x_i} + (\rho\beta)_{nf} g(T - T_C) + \frac{\partial}{\partial x_j} \left( \eta_{nf} (|\dot{\gamma}|) \frac{\partial v_j}{\partial x_i} \right) \tag{2}$$

$$(\rho c_p)_{nf} v_j \frac{\partial T}{\partial x_j} = \frac{\partial}{\partial x_j} \left( k_{nf} \frac{\partial T}{\partial x_j} \right) \tag{3}$$

where the cold-wall temperature  $T_C$  is taken to be the reference temperature for evaluating the buoyancy term  $(\rho\beta)_{nf}g(T - T_C)$  in the momentum-conservation equation.

In the momentum-balance law (Equation 2) the constitutive (i.e., rheological) equation is required for the viscous function  $\eta_{nf} (|\dot{\gamma}|)$ , which, for the power-law model, reads as:

$$\eta_{nf} (|\dot{\gamma}|) = K|\dot{\gamma}|^{n-1} \tag{4}$$

where  $|\dot{\gamma}| = \sqrt{\frac{1}{2} \sum_i \sum_j \dot{\gamma}_{ij} \dot{\gamma}_{ji}}$

is the II invariant of the symmetrical rate-of-deformation tensor with Cartesian components  $\dot{\gamma}_{ij} = (\partial v_i / \partial x_j) + (\partial v_j / \partial x_i)$ ,  $K$  is the consistency and  $n$  is the dimensionless power-law index with experimentally determined values (for a  $w = 0.4 \%$  aqueous CMC solution) of  $K = 0.048 \text{ Pas}^n$  and  $n = 0.882$ .

The relationships between the properties of the nanofluid (nf), the base fluid (bf) and pure solid (s) are given with the following empirical models<sup>4,8-13</sup>:

- Dynamic viscosity:  
 $\eta_{nf} = \eta_{bf} / (1 - \varphi)^{2.5}$
- Density:  
 $\rho_{nf} = (1 - \varphi)\rho_{bf} + \varphi\rho_s$
- Thermal expansion:  
 $(\rho\beta)_{nf} = (1 - \varphi)(\rho\beta)_{bf} + \varphi(\rho\beta)_s$
- Heat capacitance:  
 $(\rho c_p)_{nf} = (1 - \varphi)(\rho c_p)_{bf} + \varphi(\rho c_p)_s$
- Thermal conductivity:  
 $k_{nf} = k_{bf} \frac{k_s + 2k_{bf} - 2\varphi(k_{bf} - k_s)}{k_s + 2k_{bf} + \varphi(k_{bf} - k_s)}$

**Table 1:** Thermophysical properties of CMC-Au nanofluid<sup>9</sup>

**Tabela 1:** Toplotno-fizikalne lastnosti CMC-Au nanotekočine<sup>9</sup>

	$\rho$ (kg/m <sup>3</sup> )	$C_p$ (J/kg K)	$k$ (W/m K)	$\beta$ (1/K)
0.4 % CMC	997.1	4179	0.613	$2.1 \times 10^{-4}$
Au	19320	128.8	314.4	$1.416 \times 10^{-7}$

### 2.2 Geometry and boundary conditions

The simulation domain is shown schematically in **Figure 1**. The two horizontal walls of the square enlo-

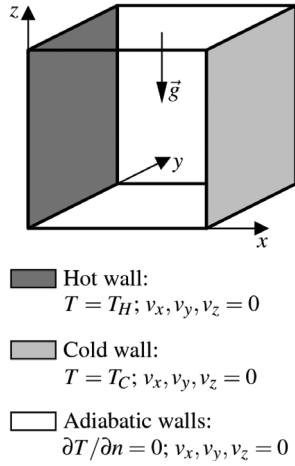


**Figure 1:** Schematic diagram of the simulation domain  
**Slika 1:** Shematski prikaz območja simulacije

sure are kept at different constant temperatures ( $T_H > T_C$ ), whereas the other boundaries are considered to be adiabatic. All the velocity components (i.e.,  $v_x$ ,  $v_y$  and  $v_z$ ) are identically zero on each boundary because of the no-slip condition and the impenetrability of the rigid boundaries.

To study the heat-transfer characteristics due to the natural convection in nanofluids, the local Nusselt number (along the vertical hot wall) is defined as<sup>15</sup>:

$$Nu(y, z) = \frac{Q_{nf, conv}}{Q_{nf, cond}} = \frac{h_{nf} L}{k_{nf}} = - \frac{L}{T_H - T_C} \left. \frac{\partial T(y, z)}{\partial x} \right|_{x=0} \quad (5)$$

where  $Nu(y, z)$  presents the ratio of the heat-transfer rate by convection to that by the conduction in the nanofluid in question,  $k_{nf}$  is the thermal conductivity and  $h_{nf}$  is the convection heat-transfer coefficient of the nanofluid:

$$h_{nf} = -k_{nf} \left. \frac{\partial T(y, z)}{\partial x} \right|_{x=0} \frac{1}{T_H - T_C} \quad (6)$$

Finally, in the present study, the heat-transfer characteristics are analysed in terms of the mean Nusselt number:

$$\overline{Nu} = \frac{1}{L^2} \int_0^L \int_0^L Nu(y, z) dy dz \quad (7)$$

and the ratio of the nanofluid heat-transfer rate to the base-fluid one:

$$\frac{Q_{nf}}{Q_{bf}} = \frac{k_{nf} \overline{Nu}_{nf}}{k_{bf} \overline{Nu}_{bf}} \quad (8)$$

at the same value of the base-fluid Rayleigh number.

In order to investigate the influence of solid-particle volume fraction  $\phi$  on the heat-transfer characteristics, the Rayleigh number ( $Ra_{nf}$ ) and Prandtl number ( $Pr_{nf}$ ) of the CMC-based nanofluid (obeying the power-law viscous behaviour) are expressed as follows:

$$Ra_{nf} = \frac{\rho_{nf} (\rho c_p)_{nf}^n g \beta_{nf} \Delta T L^{2n+1}}{k_{nf}^n K} \quad (9)$$

$$Pr_{nf} = \frac{K}{\rho_{nf}} \left( \frac{k}{\rho c_p} \right)^{n-2} L^{2-2n}$$

Using Equation 9 we show that  $Ra_{nf} < Ra_{bf}$  (**Figure 2a**) and  $Pr_{nf} < Pr_{bf}$  (**Figure 2b**) for all the values of  $\phi$ . The ratio of the CMC-based nanofluid Rayleigh and Prandtl numbers to the base-fluid Rayleigh and Prandtl numbers decreases with the increasing volume fraction of the nanoparticles; i.e., for the fixed values of  $Ra_{bf}$  and  $Pr_{bf}$ , the value of  $Ra_{nf}$  and  $Pr_{nf}$  decrease when adding nanoparticles.

### 2.3 Grid refinement and numerical accuracy

The grid independence of the present results was established with a detailed analysis using three different non-uniform meshes (the elements were concentrated towards each solid wall), the details of which are presented in **Table 2**. The table includes the numbers of the elements in a particular direction as well as the normalized minimum cell size.

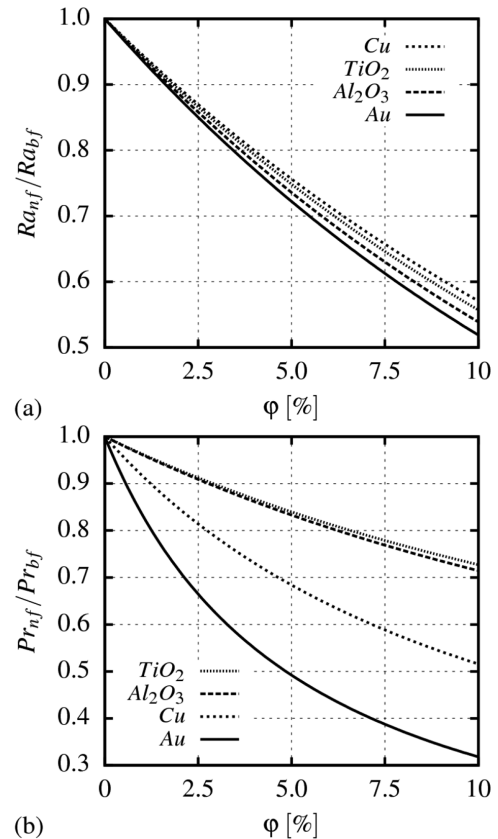


**Figure 2:** Variation of the dimensionless numbers of the CMC-based nanofluids with the volume fraction of nanoparticles: a) Rayleigh number and b) Prandtl number

**Slika 2:** Spreminjanje brezdimenzijskih števil CMC nanotekočin v odvisnosti prostorninskega deleža nanodelcev: a) Rayleighjevo število in b) Prandtlovo število

With each grid refinement the number of the elements (i.e., the control volumes) in a particular direction is increased and the element size is reduced. Such a procedure is useful for applying Richardson’s extrapolation technique (a method for obtaining a higher-order estimate of the flow value from a series of lower-order discrete values) encountered in many numerical studies<sup>8-12,17</sup>.

**Table 2:** Computational-mesh characteristics

**Tabela 2:** Značilnosti računskih mrež

	Mesh I	Mesh II	Mesh III
$N_x \times N_y \times N_z$	$40 \times 40 \times 40$	$60 \times 60 \times 60$	$90 \times 90 \times 90$
$\Delta_{min}/L$	$2.250 \times 10^{-3}$	$1.500 \times 10^{-3}$	$1.000 \times 10^{-3}$

For a general primitive variable  $\phi$  the grid-converged value (i.e., extrapolated to the zero element size) is given as<sup>8-12</sup>:  $\phi_{ext} = \phi_{M3} - (\phi_{M2} - \phi_{M3})/(r^p - 1)$  where  $\phi_{M3}$  is obtained on the basis of the finest grid and  $\phi_{M2}$  is the solution based on the next level of the coarse grid;  $r = 1.5$  indicates the ratio between the coarse- and fine-grid spacings and  $p = 2$  indicates the order of accuracy.

The numerical error  $e = |(\phi_{M2} - \phi_{ext}) / \phi_{ext}|$  for the mean Nusselt number  $\overline{Nu}$  is presented in **Table 3**. It can be seen that the differences in the grid refinement are exceedingly small and the agreement between Mesh II and the extrapolated value is extremely good (the discretisation error is below 0.20 %). Based on this estimation, the simulations in the remainder of the paper were conducted on Mesh II that provided a reasonable compromise between high accuracy and computational effort.

**Table 3:** Effect of the mesh refinement upon the mean Nusselt number ( $\varphi = 10\%$ ,  $Ra_{bf} = 10^6$ )

**Tabela 3:** Vpliv zgoščevanja mreže na srednjo vrednost Nusseltovega števila ( $\varphi = 10\%$ ,  $Ra_{bf} = 10^6$ )

Mesh I	Mesh II	Mesh III	$\overline{Nu}_{ext}$	$e$
10.075	10.089	10.095	10.099	0.109 %

### 2.4 Benchmark comparison

In addition to the aforementioned grid-dependency study, the present results were also checked against the results of other authors<sup>15,16</sup> for the natural convection of air in a cubic enclosure ( $Pr = 0.71$ ). The comparisons between the present simulation results and the corresponding benchmark values (**Table 4**) are very good and entirely consistent with our grid-dependency studies.

**Table 4:** Comparison of the present results for  $\overline{Nu}$  with the benchmark results

**Tabela 4:** Primerjava dobljenih rezultatov za  $\overline{Nu}$  z referenčnimi rezultati

	$Ra = 10^3$	$Ra = 10^4$	$Ra = 10^5$	$Ra = 10^6$
Present study	1070	2.048	4.327	8.627
Tric et al. <sup>15</sup>	1.070	2.054	4.337	8.641
Lo et al. <sup>16</sup>	1.071	2.054	4.333	8.666

## 3 RESULTS AND DISCUSSION

### 3.1 Temperature and velocity-flow field

It is useful to inspect the variations in dimensionless temperature  $\theta$  and dimensionless vertical velocity  $v_z^*$  in order to understand the influences of  $Ra_{bf}$  and  $\varphi$  on the heat-transfer characteristics during the natural convection of the CMC-Au nanofluid in the cubical enclosure.

It is evident from **Figure 3a** that the distributions of  $\theta$  become increasingly non-linear with the increasing values of  $Ra_{bf}$ . This statement is supported by the data plotted in **Figure 3b**, which demonstrates that the magnitude of the velocity component increases significantly with the increasing  $Ra_{bf}$ . For a given set of values of  $\varphi$  an increase in  $Ra_{bf}$  gives rise to a strengthening of the buoyancy forces in comparison to the viscous forces, which can be seen from **Figure 3b**, where the magnitude of  $v_z^*$  increases with the increasing  $Ra_{bf}$ . As the convective transport strengthens with the increasing  $Ra_{bf}$  the distribution of  $\theta$  becomes significantly more non-linear with the increasing  $Ra_{bf}$  (**Figure 3a**).

Furthermore, **Figure 3a** illustrates that the thermal-boundary-layer thickness next to the heated wall is influenced by the addition of nanoparticles to the base fluid. This sensitivity of the thermal-boundary-layer

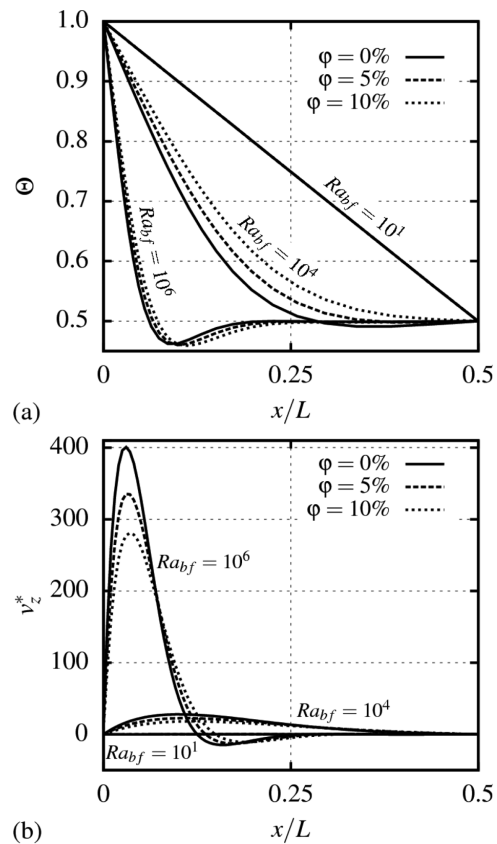


**Figure 3:** a) Variations in the non-dimensional temperature and b) non-dimensional vertical velocity component

**Slika 3:** a) Spreminjanje brezdimenzijske temperature in b) brezdimenzijske navpične komponente hitrosti

thickness to the volume fraction of the nanoparticles is related to the increased thermal conductivity of the CMC-based Au nanofluid. As a matter of fact, the increased values of the thermal conductivity are accompanied by higher values of the thermal diffusivity and these higher values of the thermal diffusivity result in a reduction in the temperature gradients and, accordingly, an increase in the thermal-boundary thickness as demonstrated in **Figure 3a**. Finally, this increase in the thermal-boundary-layer thickness reduces the Nusselt-number values.

### 3.2 Mean Nusselt number

**Figure 4** presents the variation in the mean Nusselt number with the Rayleigh number. For smaller values of the base-fluid and nanofluid Rayleigh numbers there is no convection in the nanofluid or the base fluid, and the heat transfer occurs due to pure conduction; the mean Nusselt number equals 1.0 and its value is independent of the Rayleigh number. As the value of  $Ra_{bf}$  increases, the nanofluid remains in the conductive-heat-transfer regime, while the convective-heat-transfer regime appears in the base fluid.

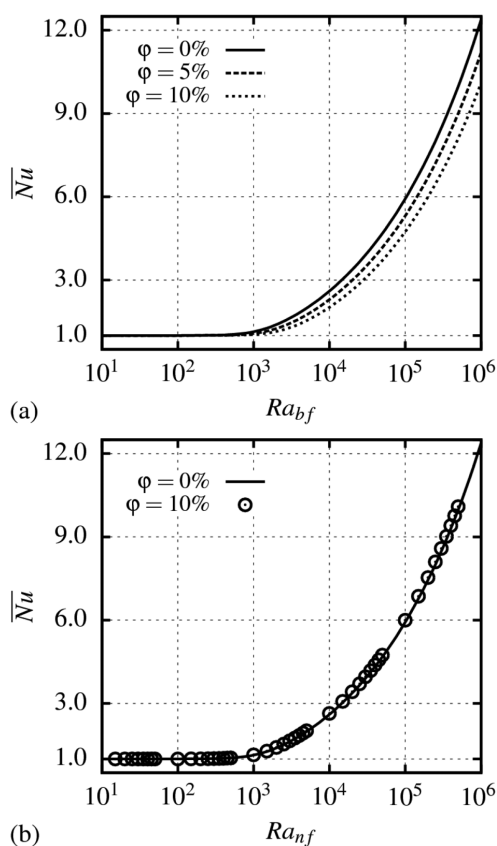


**Figure 4:** Variation in the mean Nusselt number with the: a) base-fluid Rayleigh number and b) nanofluid Rayleigh number

**Slika 4:** Spreminjanje srednjega Nusseltovega števila v odvisnosti z: a) Rayleighjevim številom nosilne tekočine in b) Rayleighjevim številom nanotekočine

The onset of the heat convection<sup>4</sup> (i.e., the critical value of the base-fluid Rayleigh number, at which the mean Nusselt number equals 1.01) depends on the volume fraction of the Au nanoparticles. The higher is the value of  $\phi$ , the more delayed is the occurrence of the convective-heat-transfer regime (**Figure 5a**). When the nanofluid is in the convective-heat-transfer regime, the mean Nusselt number monotonically increases with the Rayleigh number (**Figures 4** and **5**), attaining lower values for the higher nanoparticle volume fraction (**Figure 4**) at a given base-fluid Rayleigh number.

On the other hand, it is interesting to notice that the onset of the convection occurs at the same critical value of the nanofluid Rayleigh number, i.e.,  $Ra_{nf,cr} \cong 281$  (**Figure 5b**). Moreover, the value of the mean Nusselt number at a given nanofluid Rayleigh number is practically independent of the nanoparticle volume fraction (**Figure 4b**), which is consistent with the earlier findings in the context of the natural convection of generalized Newtonian fluids<sup>18</sup> as well as Au nanofluids<sup>4</sup> in a side wall, differentially heated, 2D square enclosure.

This finding is a reflection of the nanofluid Prandtl-number values considered in the present study and for this range of Prandtl-number values (i.e.,  $Pr_{nf} > 1$ ) the

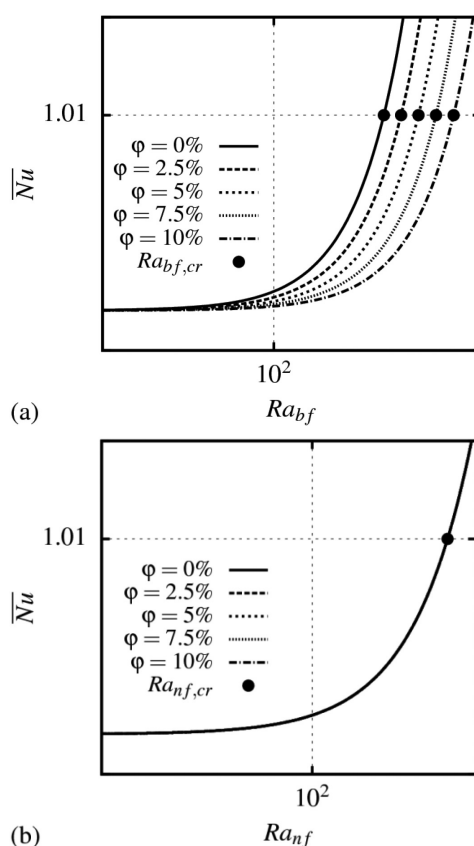


**Figure 5:** Onset of the heat-transfer convection as a function of the: a) base-fluid Rayleigh number and b) nanofluid Rayleigh number

**Slika 5:** Nastop konvektivnega prenosa toplote v odvisnosti od: a) Rayleighjevega števila nosilne tekočine in b) Rayleighjevega števila nanotekočine

hydrodynamic-boundary-layer thickness remains much greater than the thermal-boundary-layer thickness, and thus the transport characteristics are driven primarily by the buoyancy and viscous forces, which is reflected in the weak Prandtl-number dependence on the mean Nusselt number.

### 3.3 Heat-transfer rate

**Figure 6** shows the effect of the base-fluid Rayleigh number  $Ra_{bf}$  on the ratio of the heat-transfer rates for the CMC-based Au nanofluid for different values of the volume fraction.

In the range of  $Ra_{bf} \leq 281$  the heat transfer occurs due to pure conduction and the mean Nusselt number equals  $\overline{Nu} = 1$ . Consequently, the ratio of the heat transfer is equal to the ratio of thermal conductivities and it is constant and independent of the base-fluid Rayleigh number. For  $Ra_{nf} \leq 281$  and  $Ra_{bf} > 281$  the nanofluid remains in the conductive-heat-transfer regime, while the convection appears in the base fluid. The heat transfer is more important in the base fluid than in the nanofluid and the ratio of the heat-transfer rates is on a decrease.

After the onset of the convective-heat-transfer regime in the nanofluid, the ratio of the heat-transfer rates is on an increase but remains lower than the ratio obtained when both the nanofluid and the base fluid are in the conductive regime.

Last but not least, the present conclusions can be extrapolated to the other CMC-based nanofluids (e.g., Cu,  $TiO_2$  and  $Al_2O_3$ ) since their nanofluid Rayleigh- and Prandtl-number values are within the range of the present (i.e., CMC-based Au nanoparticles) Rayleigh- and Prandtl-number values.

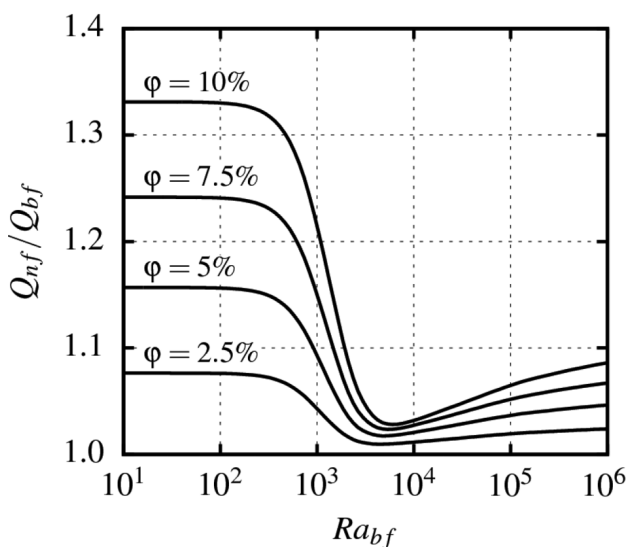


**Figure 6:** Heat-transfer rate variation with the base-fluid Rayleigh number and nanoparticle volume fraction

**Slika 6:** Spreminjanje razmerja prenosa toplote z Rayleighjevim številom nosilne tekočine in prostorninskim deležem nanodelcev

## 4 CONCLUSIONS

In the present study, a steady laminar natural convection of a non-Newtonian (i.e., CMC-based Au) nanofluid obeying the power-law rheological model in a cubical enclosure with differentially heated side walls, subjected to constant wall temperatures was analysed with numerical means. The effects of the base-fluid Rayleigh number ( $10^1 \leq Ra_{bf} \leq 10^6$ ) and the solid volume fraction ( $0\% \leq \varphi \leq 10\%$ ) on the momentum and heat-transfer characteristics were systematically investigated in detail.

The influence of the computational grid refinement on the present numerical predictions was studied throughout the examination of the grid convergence at  $Ra_{bf} = 10^6$  and  $\varphi = 10\%$ . By utilizing extremely fine meshes, the resulting discretisation error for  $\overline{Nu}$  is well below 0.2 %.

The present numerical method was validated for the case of the natural convection of air in a cubical cavity, for which the results of other authors are available in the available literature. Remarkable agreement of the present results with the benchmark results yields sufficient confidence in the presented numerical procedure and results.

Highly accurate numerical results allow some important conclusions such as:

Just after the onset of the convection, there is more heat transfer in the base fluid than in the nanofluid. At a fixed value of the base-fluid Rayleigh number  $Ra_{bf}$ , the nanofluid Rayleigh number  $Ra_{nf}$  decreases with the volume fraction of the nanoparticles. Thus, the nanoparticles delay the onset of the convection.

In the convective-heat-transfer regime the mean Nusselt number  $\overline{Nu}$  is found to increase with the increasing values of the base-fluid Rayleigh number  $Ra_{bf}$ , but the  $\overline{Nu}$  values obtained for the higher values of the nanoparticle volume fraction  $\varphi$  are smaller than those obtained in the case of the base fluid ( $\varphi = 0\%$ ) at the same nominal values of  $Ra_{bf}$ .

The transition from the conductive to the convective heat-transfer regime occurs at the same value of the nanofluid Rayleigh number, i.e.,  $Ra_{nf} \leq 281$ .

The values of the mean Nusselt number at a given  $Ra_{nf}$  are practically independent of the nanoparticle volume fraction.

The heat-transfer rate can decrease or increase depending on the value of the Rayleigh number. So, an addition of nanoparticles increases the heat transfer only for the given values of the temperature difference.

## Acknowledgements

The research leading to these results was carried out within the framework of research project "Production technology of Au nano-particles" (L2-4212) and it received the funding from the Slovenian Research Agency (ARRS).

## 5 REFERENCES

- <sup>1</sup> S. U. S. Choi, Enhancing thermal conductivity of fluids with nanoparticles, *Developments Applications of Non-Newtonian Flows*, 66 (1995), 99–105
- <sup>2</sup> W. Daungthongsuk, S. Wongwises, A critical review of convective heat transfer in nanofluids, *Renewable & Sustainable Energy Reviews*, 11 (2009), 797–817
- <sup>3</sup> F. H. Hsu, K. Wang, C. T. Huang, R. Y. Chang, Investigation on conformal cooling system design in injection molding, *Advances in Production Engineering & Management*, 8 (2013), 107–115
- <sup>4</sup> P. Ternik, R. Rudolf, Conduction and convection heat transfer characteristics of water-based Au nanofluids in a square cavity with differentially heated side walls subjected to constant temperatures, *Thermal Science*, 18 (2014), 189–200
- <sup>5</sup> G. Huelsz, R. Rechtman, Heat transfer due to natural convection in an inclined square cavity using the lattice Boltzmann equation method, *International Journal of Thermal Sciences*, 65 (2013), 111–119
- <sup>6</sup> M. N. Hasan, S. C. Saha, Y. T. Gu, Unsteady natural convection within a differentially heated enclosure of sinusoidal corrugated side walls, *International Journal of Heat and Mass Transfer*, 55 (2012), 5696–5708
- <sup>7</sup> G. Yesiloz, O. Aydin, Laminar natural convection in right-angled triangular enclosures heated and cooled on adjacent walls, *International Journal of Heat and Mass Transfer*, 60 (2013), 365–374
- <sup>8</sup> P. Ternik, R. Rudolf, Z. Žunič, Numerical study of Rayleigh-Benard natural convection heat transfer characteristics of water-based Au nanofluids, *Mater. Tehnol.*, 47 (2013) 2, 211–215
- <sup>9</sup> P. Ternik, R. Rudolf, Laminar natural convection of non-Newtonian nanofluids in a square enclosure with differentially heated side walls, *International Journal of Simulation Modelling*, 12 (2013), 5–16
- <sup>10</sup> O. Turan, R. J. Poole, N. Chakraborty, Influences of boundary conditions on laminar natural convection in rectangular enclosures with differentially heated side walls, *International Journal of Heat and Fluid Flow*, 33 (2012), 131–146
- <sup>11</sup> P. Ternik, R. Rudolf, Heat transfer enhancement for natural convection flow of water-based nanofluids in a square enclosure, *International Journal of Simulation Modelling*, 11 (2012), 29–39
- <sup>12</sup> P. Ternik, R. Rudolf, Z. Žunič, Numerical study of heat transfer enhancement of homogeneous water-Au nanofluid under natural convection, *Mater. Tehnol.*, 46 (2012) 3, 257–261
- <sup>13</sup> H. F. Oztop, E. Abu-Nada, Y. Varol, K. Al-Salem, Computational analysis of non-isothermal temperature distribution on natural convection in nanofluid filled enclosures, *Superlattices and Microstructures*, 49 (2011), 453–467
- <sup>14</sup> N. Putra, W. Roetzel, S. K. Das, Natural convection of nano-fluids, *Heat and Mass Transfer*, 39 (2002), 775–784
- <sup>15</sup> E. Tric, G. Labrosse, M. Betrouni, A first incursion into the 3D structure of natural convection of air in a differentially heated cubic cavity, from accurate numerical simulations, *International Journal of Heat and Mass Transfer*, 43 (2000), 4034–4056
- <sup>16</sup> D. C. Lo, D. L. Young, K. Murugesan, GDQ method for natural convection in a cubic cavity using velocity-vorticity formulation, *Numerical Heat Transfer, Part B*, 48 (2005), 363–386
- <sup>17</sup> I. Biluš, M. Morgut, E. Nobile, Simulation of Sheet and Cloud Cavitation with Homogenous Transport Models, *International Journal of Simulation Modelling*, 13 (2013), 94–106
- <sup>18</sup> O. Turan, A. Sachdeva, N. Chakraborty, R. J. Poole, Laminar natural convection of power-law fluids in a square enclosure with differentially heated side walls subjected to constant temperatures, *Journal of Non-Newtonian Fluid Mechanics*, 166 (2011), 1049–1063